

# A texture formation mechanism during electrodeposition

D.Y. LI, J. A. SZPUNAR

*Department of Metallurgical Engineering, McGill University, 3450 University Street, Montreal, Quebec, Canada H3A 2A7*

The texture of electrodeposited iron foil has been measured. It was observed that the deposited iron foil had a  $\{110\} \langle uvw \rangle$  type texture. If a sufficiently strong magnetic field was applied along the deposited layer during the deposition process, a  $\{110\} \langle 001 \rangle$  texture developed from the initial  $\{110\} \langle uvw \rangle$  texture, with the  $\langle 001 \rangle$  axis parallel to the direction of the applied field. An attempt has been made to explain the mechanism of texture development, as well as the effect of the magnetic field during the deposition process.

## 1. Introduction

Iron is one of the most important soft ferromagnetic materials. Various types of apparatus use iron in the form of thin laminations. Certain textures are beneficial to magnetic properties of iron sheets. However, in view of both capital and production costs in conventional manufacturing, efforts have been made to establish different methods of producing iron sheets or foils.

Much research has been performed on electrodeposited iron foils [1–9]. It was found that when the electrodeposition was carried out in a magnetic field, the iron foil formed exhibited a magnetic anisotropy which was caused by a certain texture [9]. The magnetic anisotropy is of great importance to magnetic materials. It is believed that the texture is introduced to minimize the magnetization energy in this process. But why and how the texture is formed and which parameters influence the process are unknown. It was suggested that the texture was the result of magnetostriction [10]. However, the difference of strain energies of differently oriented grains caused by magnetostriction is two orders of magnitude lower than the difference between their magnetocrystalline energies. Thus, the magnetostriction should not be the major factor dictating the formation of texture and further study is therefore needed.

In addition, we have demonstrated that the texture formed in electrodeposited iron foil without the applied magnetic field is a fibre type  $\{110\} \langle uvw \rangle$  texture. This texture is not related to the magnetic field at all. Its texture development mechanism is also unclear.

In the present paper, we have determined the texture formed in electrodeposited iron foils with and without magnetic field, and suggested a model which can be used to explain the development of texture during the electrodeposition as well as the role of the magnetic field.

## 2. Experimental procedure

The production of electrodeposited iron foils has been

described in detail elsewhere [9]. The specimens we used were 0.28 and 0.14 mm thick. They were mechanically polished and etched to remove strained layers with a solution composed of 15% HF and 85%  $H_2O_2$ . A Siemens diffractometer was used to measure their textures on both sides of the specimens. The shape and size of grains at the cross-sections of the specimens were analysed using optical metallographic techniques.

## 3. Results

Pole figures of both sides of three specimens have been measured. Specimen C was electrodeposited on a substrate of stainless steel plate. The specimen was 0.28 mm thick. Specimens A and B were electrodeposited on the same type of substrates in a magnetic field of  $132\,000 \text{ A m}^{-1}$  applied in the plane of the deposited layer along the longitudinal direction of sample A and the transverse direction of sample B, respectively. Thicknesses of A and B were 0.28 and 0.14 mm, respectively. Pole figures of C (Fig. 1a) show that the specimen has a  $\{110\} \langle uvw \rangle$  fibre texture. The texture develops quickly once the deposition takes place. This can be seen from Fig. 1a on the bottom side of sample C; a  $\{110\} \langle uvw \rangle$  texture has already formed. For specimen A which was formed in a magnetic field, its bottom side also shows a  $\{110\} \langle uvw \rangle$  texture (see Fig. 1b). However, another component of texture,  $\{110\} \langle 001 \rangle$  texture, has started to form. On the upper side, the  $\{110\} \langle 001 \rangle$  texture with the  $\langle 001 \rangle$  axis parallel to the magnetic field is well developed. Sample B reveals similar textures (Fig. 1c). On the bottom side, a  $\{110\} \langle uvw \rangle$  texture has already formed and with an increase in the thickness, a  $\{110\} \langle 001 \rangle$  texture gradually develops with the  $\langle 001 \rangle$  axis parallel to the magnetic field parallel to the transverse direction of sample B. From the above measurements, one can conclude that the  $\{110\} \langle uvw \rangle$  type texture develops first and its development is completed at a short distance from the bottom side.

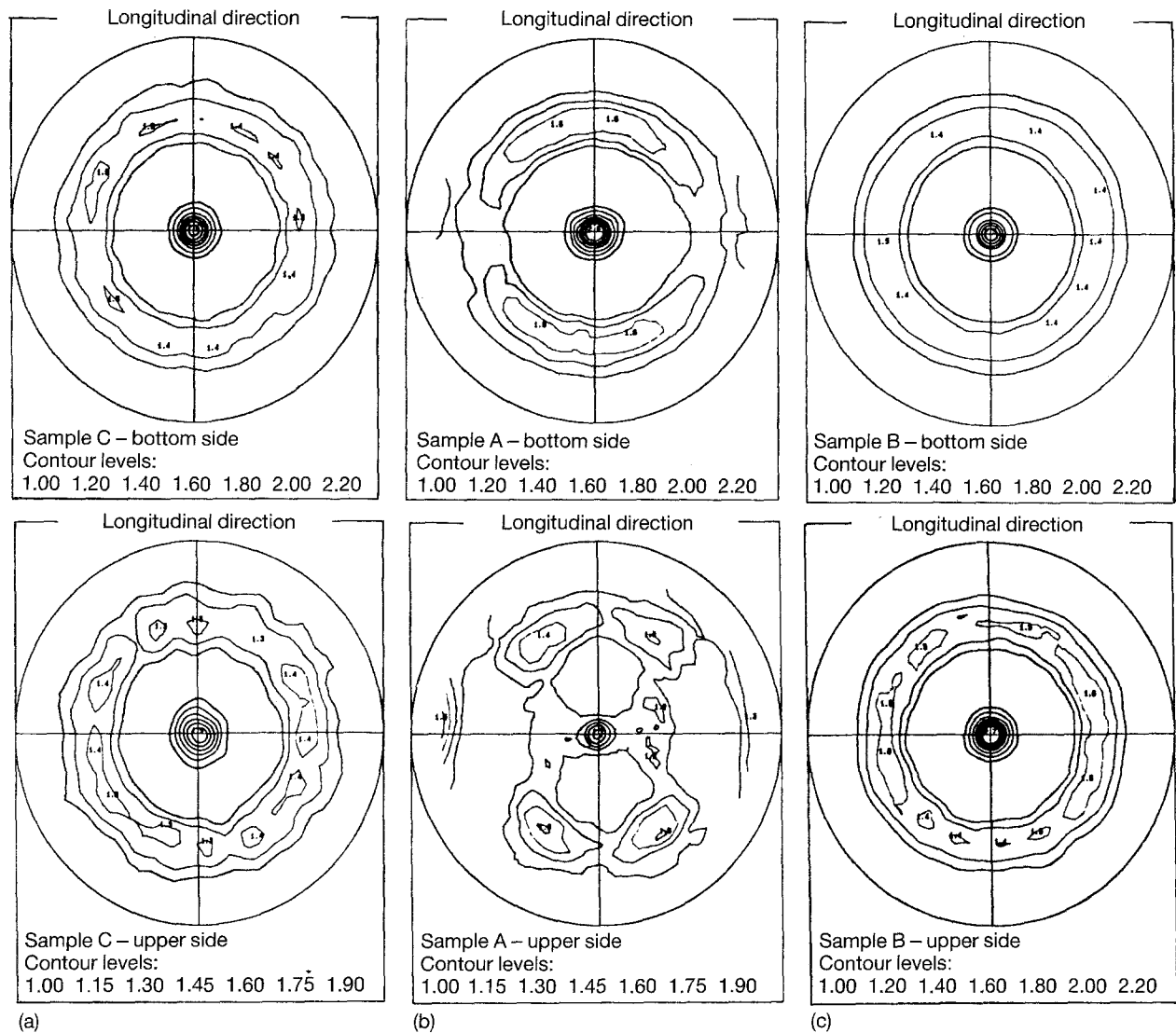


Figure 1 (a) Pole figures of sample C electrodeposited on a substrate of stainless steel. In the sample, a  $\{110\} \langle uvw \rangle$  fibre texture was formed. Sample C is 0.28 mm thick. (b) Pole figures of sample A which was deposited in a magnetic field of  $132000 \text{ A m}^{-1}$ . On the bottom side, a  $\{110\} \langle uvw \rangle$  fibre texture exists and the  $\{110\} \langle 001 \rangle$  texture starts to form with the  $\langle 001 \rangle$  axis parallel to the field. On the upper side, the  $\{110\} \langle 001 \rangle$  texture is well developed. Sample A is 0.28 mm thick. (c) Pole figures of sample B deposited in a magnetic field of  $132000 \text{ A m}^{-1}$  which was parallel to the transverse direction of the sample. A  $\{110\} \langle uvw \rangle$  fibre texture was formed and on the upper side, a weak  $\{110\} \langle 001 \rangle$  texture component can be seen. The sample is 0.14 mm thick.

If a magnetic field is applied in the plane of the deposited layer during the deposition process, a  $\{110\} \langle 001 \rangle$  texture will develop gradually from the initially formed  $\{110\} \langle uvw \rangle$  texture which dominates the layers close to the substrate. This phenomenon can be observed by comparing the pole figures of samples A and B measured on the upper side layer. On the bottom sides of both samples A and B,  $\{110\} \langle uvw \rangle$  type texture has already formed. On the upper side of sample A, the  $\{110\} \langle 001 \rangle$  texture has replaced the  $\{110\} \langle uvw \rangle$  texture, while on the upper side of sample B, which is only half the thickness of sample A, the  $\{110\} \langle 001 \rangle$  component is weak.

The microstructures at cross-sections of all specimens were studied with an optical microscope. Fig. 2 shows the cross-section of sample C. There is a large number of fine grains on the bottom side. As the thickness increases and exceeds 0.02 mm, the grains become bigger and longer, and consequently the number of grains decreases. On the bottom of the specimen, there is competition between the differently

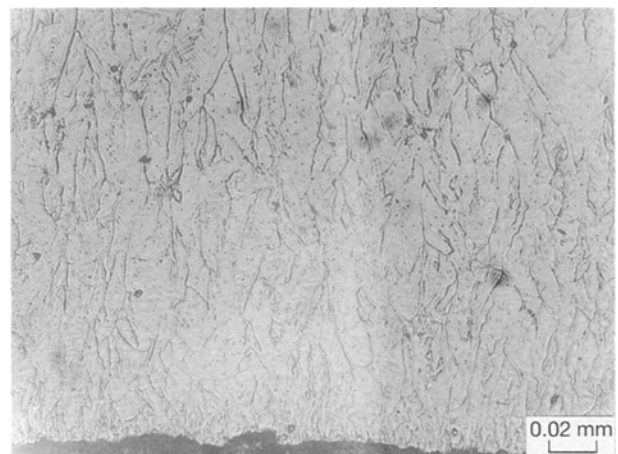


Figure 2 Microstructure of the cross-section of sample C.

oriented grains. Some grow continuously (Fig. 3) and others are prevented from growing by more competitive neighbouring grains. According to our texture measurements, the faster growing grains are those

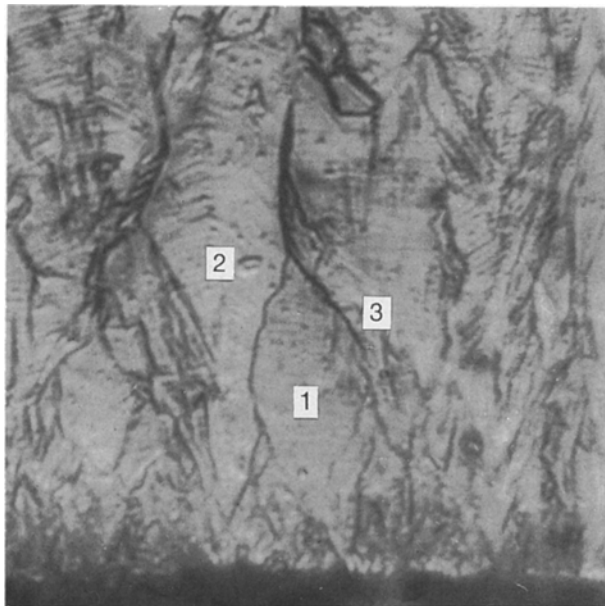


Figure 3 Microstructure of the cross-section of sample C ( $\times 1250$ ) showing that as the thickness of the foil increases, certain grains are covered by neighbouring grains.

having  $\{110\}$  crystallographic planes parallel to the foil surface. From the point of view of thermodynamics, the energy introduced by the growth of grains with  $\{110\}$  planes parallel to the foil surface must be lower than that introduced by the growth of other grains. Samples A and B were also analysed. They have microstructures similar to that of sample C.

#### 4. The model of texture development and discussion of results

The mechanism of the formation of  $\{110\} \langle uvw \rangle$  fibre texture is not clear. Because the iron nucleates on the substrate, it is reasonable to consider two possible reasons for the formation of  $\{110\} \langle uvw \rangle$  texture: one is the influence of the substrate and another the selected grain growth related to the surface energy.

The substrate might influence the nucleation in the iron foil at the beginning of the deposition process, because grains of the substrate might generate nuclei of such orientation which satisfies the condition of minimum interfacial energy. This type of texture should inherit certain characteristics from the substrate. For instance, the texture formed in the iron foil should have the same symmetry as the texture in the substrate. In our case, the substrate is a stainless steel plate in which a typical texture is  $\{111\} \langle 211 \rangle$  [11]. However, in the deposited iron foil, the  $\{110\}$  planes are aligned parallel to the foil surface but the grain orientation exhibits axial symmetry which does not reflect the texture symmetry in the substrate of stainless steel at all. Therefore, we can conclude that the texture in the deposited iron foil is not induced by the texture of the substrate. This influence of the substrate might be a good reason in the nucleation stage at the beginning of the deposition process, but it is not applicable in the grain growth stage which plays a

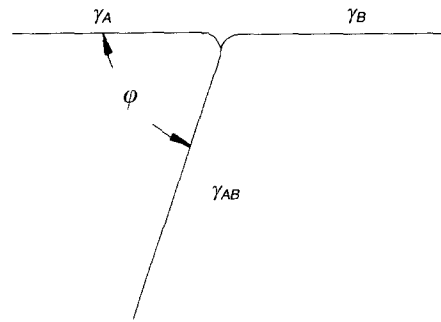


Figure 4 Schematic view of the cross-section of two neighbouring grains.

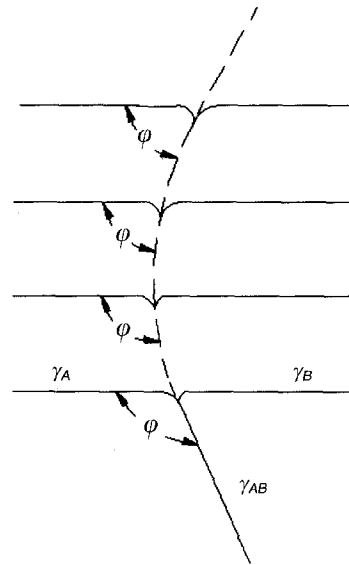


Figure 5 Schematic illustration of the formation of a grain boundary in the deposition process. The boundary bends to reach the equilibrium state.

decisive role in the formation of the  $\{110\} \langle uvw \rangle$  texture.

The surface energy could also be responsible for the formation of the  $\{110\} \langle uvw \rangle$  texture. It is known that this energy is the main parameter controlling grain growth [12–14]. A well-known equilibrium condition is [12]

$$\cos\phi = \frac{\gamma_B - \gamma_A}{\gamma_{AB}} \quad (1)$$

where  $\gamma_A$  and  $\gamma_B$  are surface energies of two neighbouring grains, and  $\gamma_{AB}$  is the interfacial energy of the grain boundary between them (see Fig. 4). If  $\gamma_B > \gamma_A$ , the equilibrium state requires  $\phi < \pi/2$ , which makes grain A grow preferentially. Equation 1 also describes the equilibrium conditions for grain growth in the deposition process. Fig. 5 schematically illustrates changes which occur at various stages of grain growth. Consider a case where two neighbouring grains are in a non-equilibrium state and suppose that  $\phi > \cos^{-1}[(\gamma_B - \gamma_A)/\gamma_{AB}]$ . When iron ions arrive in the vicinity of the junction where surfaces A and B and the grain boundary AB meet, the deposited ion will settle so that the equilibrium state is achieved. Therefore, with increasing thickness of the foil, the angle  $\phi$  will decrease until it reaches the equilibrium angle

given by Equation. 1. In this process, the junction moves towards the grain with higher surface energy,  $\gamma_B$ , and consequently the newly formed segment of the grain boundary AB is bent (Fig. 5). In consequence, the grain with the higher surface energy,  $\gamma_B$ , will gradually be covered by the grain with the lower surface energy,  $\gamma_A$ , as the thickness of the foil increases, i.e. the grain with the lower surface energy grows preferentially. The surface energies of different crystallographical planes of iron and the interfacial energy of the grain boundary, derive from the theoretical calculation and the experimental work [15, 16]. Of all the crystallographic planes of iron, the  $\{110\}$  plane has the lowest surface energy. The average value of the difference between the surface energies of the  $\{110\}$  plane, and the  $\{hkl\}$  plane can be estimated according to the previous work [15, 16]. Therefore, the average  $\phi$  can be evaluated using Equation 1 as equal to  $64^\circ$ . With this equilibrium angle, the grain having the  $\{110\}$  crystallographical plane parallel to the foil surface grows and expands until it meets similar type grains which are nearby and grow similarly. Consequently, grains between them are covered (Fig. 3: grain 1 is covered by grains 2 and 3). The grains which are very small at the beginning of the deposition can easily be covered by the  $\{110\}$   $\langle uvw \rangle$  type grains. This process is almost completed within a layer about 0.02 mm thick (Fig. 2). This is the reason why, on the bottom side of the iron foils, the  $\{110\}$   $\langle uvw \rangle$  type texture is already well developed. Once the  $\{110\}$   $\langle uvw \rangle$  grains are dominant, grain boundaries become straighter and longer, because there is no difference in surface energies between  $\{110\}$   $\langle uvw \rangle$  grains.

The lowest surface energy of the  $\{110\}$  planes leads to a  $\{110\}$   $\langle uvw \rangle$  type texture, but when a magnetic field is applied along the direction parallel to the surface of the deposited layer, a  $\{110\}$   $\langle 001 \rangle$  texture develops.

The competition between differently oriented grains in the magnetic field is attributed to differences in their magnetic energies, in addition to differences of their surface energies analysed earlier. Different grain magnetic energies are attributed to two components, the magnetocrystalline anisotropy and the magnetostriction anisotropy. The former represents the difference in magnetization energies between different crystallographic directions of a crystal. The latter refers to differences in the state of strain in the external magnetic field [17]. The difference in magnetocrystalline energies between differently oriented grains is about  $10^5$  erg  $\text{cm}^{-3}$ , ( $10^{-7}$  erg = 1 J) while the difference of the strain energies is  $10^2$ – $10^3$  erg  $\text{cm}^{-3}$ . We can therefore neglect the magnetostriction and only consider the magnetocrystalline anisotropy which, for cubic crystals, is expressed as [17]

$$E_a = K_1(\alpha_1^2\alpha_2^2 + \alpha_2^2\alpha_3^2 + \alpha_3^2\alpha_1^2) + K_2(\alpha_1^2\alpha_2^2\alpha_3^2) \quad (2)$$

where  $\alpha_1$ ,  $\alpha_2$  and  $\alpha_3$  are direction cosines of the angles between the direction of magnetization and the three axes of the crystal reference frame.  $K_1$  and  $K_2$  are the magnetocrystalline anisotropy constants. For iron,  $\langle 001 \rangle$  axis is the easy magnetization axis. The free

energy is the lowest if the magnetic field is parallel to the easy axis of the iron crystal. Grains having lower free energies can grow in the deposition process faster than those having higher free energies. In our case, the competition between differently oriented grains depends upon both the free energy and the surface energy.

To determine how the texture develops as a result of this competition, let us first consider a bicrystal in a magnetic field (Fig. 6). Volumetric free energies related to the magnetocrystalline anisotropy, of crystals 1 and 2 are different. Suppose  $f_1 < f_2$ ; according to the law of thermodynamics, crystal 1 will grow by consuming crystal 2 and the free energy of the whole system will decrease. Let crystal 1 increase its volume by  $dV = dl dS$ , here  $dS$  represents an area of grain boundary which moves a distance of  $dl$ . The change in the free energy of crystal 1 will be  $(f_2 - f_1)dV$ . If we assume that there is a pressure,  $P$ , which is responsible for the grain-boundary movement, the work needed to increase the grain volume can be expressed as  $(P dS)dl$  which should be equal to the change of the free energy, that is

$$(P dS)dl = (f_2 - f_1)dV = \Delta f dS dl \quad (3)$$

We thus obtain

$$P = \Delta f = (f_2 - f_1) \quad (4)$$

This means that the driving force for the grain-boundary migration is due to the difference of free energies and can be described by a pressure,  $P$ .

As mentioned earlier in the discussion of the electrodeposition of iron foil, the equilibrium angle,  $\phi$ , given by Equation 1 is reached when the surface energies and the interfacial energy of the grain boundary are in equilibrium. When a magnetic field is applied, the pressure,  $P$ , acting on the grain boundary must be considered. Fig. 7 illustrates the equilibrium state when the surface energy,  $\gamma_A$  and  $\gamma_B$ , grain boundary energy,  $\gamma_{AB}$ , and the pressure,  $P$ , from the magnetocrystalline anisotropy are involved. Once the field is applied, the pressure,  $P$ , makes the grain boundary tend to bend. The larger is the difference in the magnetization energy, i.e. the larger is the pressure,  $P$ , the greater is the tendency of bending. Fig. 7 shows that because of pressure,  $P$ , the direction of the grain-boundary tension, i.e.  $\gamma_{AB}$ , tends to deviate from its

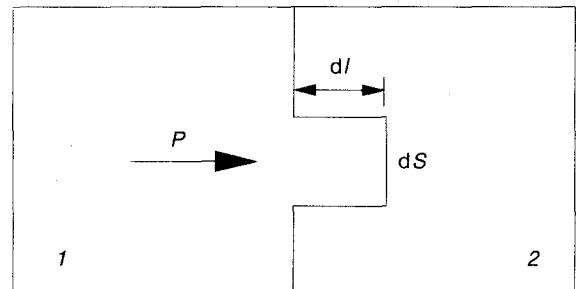


Figure 6 A bicrystal in a magnetic field. Suppose the magnetic free energy per volume of crystal 1 is smaller than that of crystal 2 due to the magnetocrystalline anisotropy, a pressure,  $P$ , exists and pushes the grain boundary to move towards crystal 2.

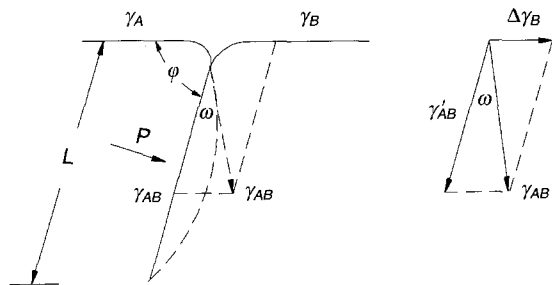


Figure 7 In a magnetic field, equilibrium is reached when the surface energy,  $\gamma_A$  and  $\gamma_B$ , the interfacial energy of grain boundary,  $\gamma_{AB}$ , and the pressure,  $P$ , are in equilibrium.

original direction by an angle  $\omega$ . If we breakdown  $\gamma_{AB}$  into two components,  $\gamma'_{AB} = \gamma_{AB}(\cos\omega + \sin\omega \text{ctg}\phi)$  and  $\Delta\gamma_B = \gamma_{AB} \sin\omega/\sin\phi$ , which are respectively parallel to the original direction of  $\gamma_{AB}$  and that of  $\gamma_B$  and then substitute into Equation 1  $\gamma_B + \Delta\gamma_B$  for  $\gamma_B$  and  $\gamma'_{AB}$  for  $\gamma_{AB}$ , the equilibrium equation for the surface energy, the grain-boundary energy and the magnetic free energy are obtained, thus

$$\begin{aligned} \cos\phi &= [(\gamma_B + \Delta\gamma_B) - \gamma_A]/\gamma'_{AB} \\ &= [(\gamma_B - \gamma_A)/\gamma_{AB} + \sin\omega/\sin\phi]/ \\ &(\cos\omega + \sin\omega \text{ctg}\phi) \end{aligned} \quad (5a)$$

and

$$\sin\omega = L(P/2\gamma_{AB}) \quad (5b)$$

where  $L$  is the length of the grain.  $\phi$  is the angle between the grain boundary and the surface A (Fig. 7).

The surface energy and the magnetic free energy are two independent parameters. Whether the magnetic field is applied or not, the  $\{110\}$  crystallographic plane which has the lowest surface energy is always parallel to the sample surface. On the other hand, the orientation of grains having  $\{110\}$  planes parallel to the specimen surface is only influenced by the magnetic field. When a magnetic field is applied, those  $\{110\} \langle uvw \rangle$  grains, which have their easy magnetization axes  $\langle 001 \rangle$  parallel to the field will grow preferentially.

Numerical evaluation of an average equilibrium angle,  $\phi$ , between the  $\{110\} \langle uvw \rangle$  grain and grains which are randomly oriented, and that exist between a  $\{110\} \langle 001 \rangle$  grain and grains having random orientations, has been made using Equation 5. In this evaluation the average value of the difference in surface energies between  $\{110\} \langle uvw \rangle$  grains and randomly oriented grains, as well as that of the magnetic free energies between  $\{110\} \langle 001 \rangle$  grains and randomly oriented grains, are estimated using available experimental data and theoretical calculations [15, 17]. Results have been schematically illustrated in Fig. 8.

Fig. 8a represents the angle  $\phi$  between the  $\{110\} \langle uvw \rangle$  grain and other types of grains versus the grain length. In the same figure,  $\phi$  between the  $\{110\} \langle 001 \rangle$  grain and other grains in a magnetic field strong enough to saturate the specimen, is also presented. There is no significant difference between these two curves when the grain length is less than 0.03 mm.

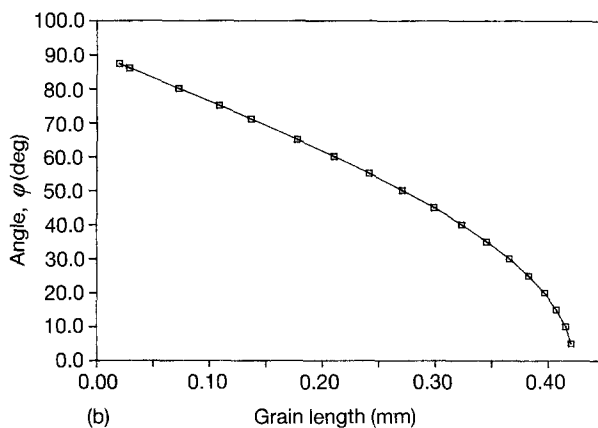
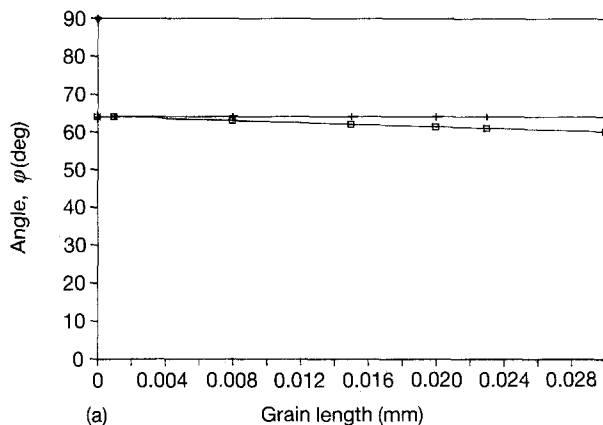


Figure 8 (a) (+) The average angle,  $\phi$ , between the  $\{110\} \langle uvw \rangle$  grain and other grains, ( $\square$ )  $\phi$  between a  $\{110\} \langle 001 \rangle$  grain and others, versus the grain length in a magnetic field strong enough to saturate the iron. (b) The angle  $\phi$  between  $\{110\} \langle 001 \rangle$  grains and  $\{110\} \langle uvw \rangle$  grains as a function of the grain length.

Fig. 8b shows  $\phi$  between  $\{110\} \langle 001 \rangle$  and  $\{110\} \langle uvw \rangle$  grains with the grain length. It can be seen from the figure that at the beginning of the deposition,  $\phi$  between  $\{110\} \langle 001 \rangle$  and  $\{110\} \langle uvw \rangle$  grains is  $90^\circ$ , which implies that these two types of grain have equal growth rates. With increasing grain length,  $\phi$  decreases. As a result,  $\{110\} \langle 001 \rangle$  grains grow faster and the  $\{110\} \langle 001 \rangle$  texture becomes stronger and dominates the  $\{110\} \langle uvw \rangle$  texture. According to Fig. 8a and b, at the beginning of the deposition in a magnetic field the  $\{110\} \langle uvw \rangle$  type grains including  $\{110\} \langle 001 \rangle$  grains having  $\phi = 64^\circ$  grow and cover other grains rather quickly. With increasing grain length, the growth of  $\{110\} \langle 001 \rangle$  grains becomes faster than other  $\{110\} \langle uvw \rangle$  grains and, in consequence, the  $\{110\} \langle 001 \rangle$  texture develops. Therefore, it is understandable that in the experiment we observed the  $\{110\} \langle uvw \rangle$  texture close to the substrate, while on the upper side of the specimen the  $\{110\} \langle 001 \rangle$  texture showed up (Fig. 1b). At the beginning of deposition, the grain length,  $L$ , is small and therefore the influence of magnetic field is small (Equation 5). In our experiment we can see that the development of  $\{110\} \langle 001 \rangle$  texture is initially slow and becomes faster as the thickness of the iron foil increases, i.e. comparing Fig. 1c and b we see that the

{110} <001> texture is very weak in sample B (thickness 0.14 mm) while sample A, whose thickness is twice that of sample B, has a stronger {110} <001> texture.

It should be pointed out that evaluation of the equilibrium angle,  $\phi$ , is not accurate because the surface energy possibly changes in the electrolyte during the electrodeposition process. Also the experimental data on the surface energy of iron are limited. In order to obtain a better understanding of the process, further research on the surface energy in this specific case is needed.

## 5. Conclusion

The electrodeposited iron foil has a {110}  $\langle uvw \rangle$  type texture. This texture might be attributed to the lowest surface energy of {110} crystallographical planes of iron. If a magnetic field is applied parallel to the surface of the deposit during the deposition process, a {110} <001> texture develops with the <001> axis parallel to the direction of the applied magnetic field. In this case, both the surface energy and the magnetic free energy are responsible for the development of the texture.

## Acknowledgements

The authors thank Mr A. Rugege for specimens used in this research, and Mr S. Poplawski for texture measurements. We also acknowledge the financial support of the Natural Science and Engineering Research Council of Canada.

## References

1. S. F. HARTY, J. A. McGEOUGH and R. M. TULLOCH, *Surface Technol.* **12** (1981) 39.
2. H. E. CLEAVES and J. G. THOMPSON, "The Metal-Iron", 1st Edn (McGraw-Hill, New York, 1935).
3. I. W. WOLF, *J. Electrochem. Soc.* October **108** (1961) 959.
4. E. RAUB and K. MÜLLER, "Fundamentals of Metal Deposition" (Elsevier, New York, 1967).
5. N. V. PARTHASARADHY, "Practical Electroplating Handbook" (Prentice Hall, Englewood, New Jersey, 1989).
6. W. A. CRICHTON, J. A. McGEOUGH and J. R. THOMSON, *J. Mech. Eng. Sci.* **22** (2) (1980) 49.
7. I. B. MácCORMACK, W. D. CORNER and B. K. TANNER, *IEEE Trans. Mag.* **Mag-17** (1981) 2940.
8. S. H. F. LAI and J. A. McGEOUGH, *J. Mech. Eng. Sci.* **18** (1976) 19.
9. Munny'Mbabazi A. RUGEGE, Master thesis, University of Aberdeen, December 1983.
10. N. V. KOTEL'NIKOV, *Fiz. Metal. Metalloved* **6** (1958) 222.
11. C. B. BARRETT and T. B. MASSALSKI, "Structure of Metals", 3rd revised Edn, (McGraw-Hill, New York, 1966) Ch. 21.
12. J. L. WALTER and C. G. DUNN, *AIME Trans.* **215** (1959) 465.
13. E. D. HONDROS and L. E. H. STUART, *Philos. Mag.* **17** (1968) 711.
14. J. L. WALTER and C. G. DUNN, *Acta. Metall.* **8** (1960) 497.
15. LAWRENCE E. MURR, "Interfacial Phenomena in Metals and Alloys" (Addison-Wesley, Advanced Book Program, Reading, MA, 1975).
16. J. K. MACKENZIE, A. J. W. MOORE and J. F. NICHOLAS, *J. Phys. Chem. Solids* **23** (1962) 185.
17. C. W. CHEN, "Magnetism and Metallurgy of Soft Magnetic Materials" (North-Holland, New York, 1977) p. 61.

Received 12 May 1992  
and accepted 11 March 1993